

EFFECTS OF THERMAL AND MASS STRATIFICATION ON UNSTEADY MHD FLOW PAST AN OSCILLATING VERTICAL PLATE EMBEDDED IN A POROUS MEDIUM WITH VARIABLE SURFACE CONDITIONS

 Pappu Das*,  Rudra Kanta Deka

Department of Mathematics, Gauhati University, Guwahati-781014, Assam, India

*Corresponding Author e-mail: pappudas751@gmail.com

Received June 2, 2024; revised July 16, 2024; accepted July 29, 2024

Investigations have been made into how thermal and mass stratification affect the magnetohydrodynamic flow past a plate which is oscillating vertically in its own axis in which it is embedded in a porous medium with variable heat and mass diffusion. For concentration, temperature and velocity fields, the non-dimensional governing equations are solved using the Laplace transform method for the unitary Prandtl and Schmidt numbers, when the plate is oscillating in its own plane harmonically. Numerical computations are carried out and presented in graphs for different physical parameters like thermal Grashof number, phase angle, mass Grashof number, stratification parameter and time on concentration, velocity, temperature, plate heat flux, mass flux and skin friction. The findings of this study can be utilized to enhance comprehension of MHD flow on vertical oscillating plate in combined stratified environments. Significant findings arising from the mass and thermal stratification are compared to the scenario in which stratification is absent.

Keywords: *MHD flow; Oscillating plate; Electrically conducting fluid; Unsteady flow; Thermal stratification; Mass stratification; Porous medium*

PACS: 44.05.+e, 47.11.-j, 47.55.P-, 47.56.+r, 47.65.-d

1. INTRODUCTION

When two types of stream with different temperatures come into contact, thermal stratification happens. A colder, denser layer is covered by a warmer, less dense layer in a process known as thermal stratification of fluid, which occurs naturally at higher temperatures. It happens mostly as a result of changes in temperature, concentration, or the presence of various fluids with differing densities. Between cold and hot fluid zones, this natural mechanism produces a temperature gradient transition zone. Because of its numerous widespread applications in a variety of industrial, engineering, and environmental applications, the dynamics of thermally stratified fluid has recently caught the attention of researchers and emerged as an important area for scientific inquiry. Engineering problems like electromagnetic casting, liquid-metal cooling of nuclear reactors, and plasma confinement are all related to magnetohydrodynamic flow.

MHD flow under thermal and mass stratification effects have been a topic of great interest for the last three decades. Many authors have been studied MHD flow past vertical plates and cylinders with stratification effects. Some of the authors are Soundalgekar *et. al.* [1], Park and Hyun [2], Das *et. al.* [3]. Natural convection of a viscous stratified fluid in one dimension was studied by Park and Hyun [2] and Park [4]. Shapiro and Fedorovich [5] studied thermally stratified fluid flows through vertical plates and cylinders under various surface conditions and by include the stratification parameter in the energy equation, they have recently improved the classical theory of one-dimensional flow. In contrast with using the similarity transformation method, Magyari *et. al.* [6] investigated the unstable free convection flow along an infinite vertical flat plate embedded in a stably stratified fluid-saturated porous media. [7] and [9] investigated the effects of thermal and mass stratification in non-Newtonian fluid saturated porous media along a vertical wavy truncated cone and a vertical wavy surface respectively. [8] came up with an analytical solution of MHD heat and mass diffusion flow by natural convection past a surface embedded in a porous medium. Analytical solution for unsteady natural convection flow past an accelerated vertical plate in a thermally stratified fluid was given by [10]. Under MHD conditions, the impact of a thermally stratified ambient fluid along a moving non-isothermal vertical plate was examined by [11]. [12] studied how a transverse magnetic field effects the flow of a convectively driven flow immersed in a fluid with stable stratification along an infinite vertical plate. [13] investigated the radiative flow past an exponentially accelerated vertical plate with variable temperature and mass diffusion. Under MHD free convection the effects of chemical reaction and radiation was studied by [14] when the flow past an exponentially accelerated vertical plate with variable temperature and variable mass diffusion. Effects of thermal and mass stratification on convectively driven flow past an infinite moving vertical cylinder was studied by [15]. [16] came up with the closed form solution of thermal and mass stratification effects on unsteady flow past an accelerated infinite vertical plate with variable temperature and exponential mass diffusion in porous medium. The effects of thermal and mass stratification on unsteady parabolic flow past an infinite vertical plate with exponential decaying temperature and variable mass diffusion in porous medium was studied by [17]. [18] conducted research on thermal and mass stratification effects on MHD nanofluid past an exponentially accelerated vertical plate through a porous medium

with thermal radiation and heat source. Theoretical study of thermal and mass stratification effects on MHD nanofluid past an exponentially accelerated vertical plate in a porous medium in presence of heat source, thermal radiation and chemical reaction were done by [19]. [20] and [21] came up with the solutions of thermal and mass stratification impacts on unsteady MHD flow with different conditions. [22] looked at the influences of thermal stratification and chemical reaction on MHD free convective flow along an accelerated vertical plate with variable temperature and exponential mass diffusion in a porous medium.

In this article, we investigate the impacts of thermal and mass stratification on MHD flow through a plate which is oscillating vertically in its own axis and is embedded in a porous medium with variable surface conditions. In this case, the term known as pressure work is included in the thermodynamic energy equation, the consideration of thermal and mass stratification. For the unit Prandtl and Schmidt numbers the solutions are then obtained. The investigation on velocity, temperature and concentration profiles are made under the impacts of variables and displayed on graphs. These variables include the thermal Grashof number Gr , mass Grashof number Gc , magnetic parameter M , time t , permeability of the porous medium K and stratification parameters γ and ξ . On other physical phenomena including the rate of heat and mass transfer and skin friction, the effects of M , Gr , Gc , γ , ξ and t are also studied.

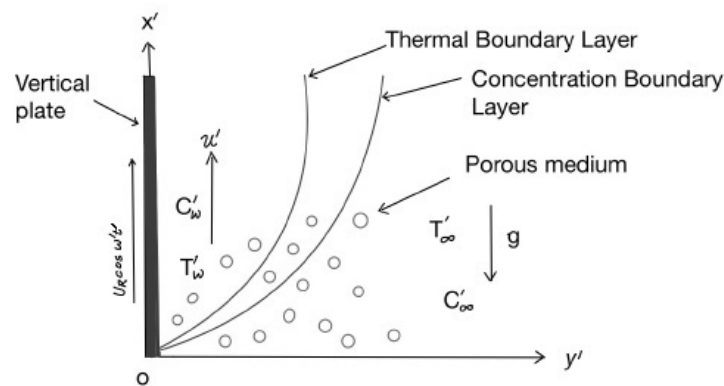


Figure 1. Physical Model and Coordinate System

2. MATHEMATICAL ANALYSIS

In our study an incompressible, viscous and electrically conducting fluid along an oscillating vertical plate that is embedded in a porous medium with variable surface conditions in two dimensional flow is examined. The plate is taken along the x' -axis, and the y' -axis is taken normal to it. At the beginning, the fluid and the plate have the same temperature T'_∞ and concentration C'_∞ throughout. The plate begins oscillating in its own plane at time t' , moving with a velocity $U_R \cos \omega't'$, the concentration level at the plate is raised to C'_w and the plate temperature is raised to T'_w . In order to ignore the induced magnetic field, a uniformly strong magnetic field is applied perpendicular to the plate with a modest magnetic Reynolds number. Following these conditions, the equations for motion, energy and concentration are represented using the Boussinesq's approximation as follows:

$$\frac{\partial u'}{\partial t'} = \nu \frac{\partial^2 u'}{\partial y'^2} + [g\beta(T' - T'_\infty) + g\beta_c(C' - C'_\infty)] - \frac{\sigma B_0^2 u'}{\rho} - \frac{\nu u'}{k'} \quad (1)$$

$$\frac{\partial T'}{\partial t'} = \frac{k}{\rho C_p} \frac{\partial^2 T'}{\partial y'^2} - \gamma' u' \quad (2)$$

$$\frac{\partial C'}{\partial t'} = D \frac{\partial^2 C'}{\partial y'^2} - \xi' u' \quad (3)$$

Considering the initial and boundary conditions as:

$$u' = 0, \quad T' = T'_\infty, \quad C' = C'_\infty \quad \forall y', t' \leq 0$$

$$u' = U_R \cos \omega't', \quad T' = T'_\infty + (T'_w - T'_\infty)At',$$

$$C' = C'_\infty + (C'_w - C'_\infty)At' \quad \text{at } y' = 0, \quad t' > 0 \quad (4)$$

$$u' \rightarrow 0, \quad T' \rightarrow T'_\infty, \quad C' \rightarrow C'_\infty \quad \text{as } y' \rightarrow \infty, \quad t' > 0$$

Now, we introduce the following non-dimensional quantities:

$$y = \frac{y'}{L_R}, \quad t = \frac{t'}{t_R}, \quad u = \frac{u'}{U_R}, \quad Da = \frac{U_R^2 k'}{\nu^2}, \quad \omega = \omega' t_R, \quad Pr = \frac{\mu C_p}{k}$$

$$M = \frac{\sigma B_0^2 \nu}{\rho U_R^2}, \quad Sc = \frac{\nu}{D}, \quad \theta = \frac{T' - T'_\infty}{T'_w - T'_\infty}, \quad C = \frac{C' - C'_\infty}{C'_w - C'_\infty}, \quad \Delta T = T'_w - T'_\infty \quad (5)$$

$$Gc = \frac{\nu g \beta_c (C'_w - C'_\infty)}{U_R^3}, \quad U_R = (\nu g \beta \Delta T)^{1/3}, \quad L_R = \left(\frac{g \beta \Delta T}{\nu^2} \right)^{-1/3}, \quad A = \frac{1}{t_R},$$

$$t_R = (g \beta \Delta T)^{-2/3} \nu^{1/3}, \quad Gr = \frac{\nu g \beta (T'_w - T'_\infty)}{U_R^3}, \quad \gamma = \frac{\gamma' L_R}{\Delta T}, \quad \xi = \frac{\xi' L_R}{C'_w - C'_\infty}$$

The following forms are taken by equations (1), (2) and (3) when the non-dimensional quantities defined in (5) above are used,

$$\frac{\partial u}{\partial t} = \frac{\partial^2 u}{\partial y^2} + Gr\theta + GcC - \left(M + \frac{1}{Da} \right) u \quad (6)$$

$$\frac{\partial \theta}{\partial t} = \frac{1}{Pr} \frac{\partial^2 \theta}{\partial y^2} - \gamma u \quad (7)$$

$$\frac{\partial C}{\partial t} = \frac{1}{Sc} \frac{\partial^2 C}{\partial y^2} - \xi u \quad (8)$$

And the corresponding initial and boundary conditions (4) then reduce to,

$$u = 0, \quad \theta = 0, \quad C = 0 \quad \forall y, \quad t \leq 0$$

$$u = \cos \omega t, \quad \theta = t, \quad C = t \quad \text{at } y = 0, \quad t > 0 \quad (9)$$

$$u \rightarrow 0, \quad \theta \rightarrow 0, \quad C \rightarrow 0 \quad \text{as } y \rightarrow \infty, \quad t > 0$$

2.1. Method of Solution

With respect to the boundary conditions (9), the non-dimensional governing equations (6), (7), and (8) are solved using the Laplace transform technique for the tractable cases $Pr = 1$ and $Sc = 1$. The expression for velocity, temperature and concentration profiles are obtained with the help of [23] are as follows,

$$u = C_1 [f_1(A, -i\omega) + f_1(A, i\omega)] - C_2 [f_1(B, -i\omega) + f_1(B, i\omega)] - C_3 [f_2(A) + f_2(B)] \quad (10)$$

$$\theta = t(1 + D_1 - D_2) \left\{ \left(1 + \frac{y^2}{2t} \right) \operatorname{erfc} \left(\frac{y}{2\sqrt{t}} \right) - \frac{ye^{-\frac{y^2}{4t}}}{\sqrt{\pi t}} \right\}$$

$$+ \frac{\gamma}{2(A - B)} [f_1(A, -i\omega) + f_1(A, i\omega) - f_1(B, -i\omega) - f_1(B, i\omega)] - \frac{D_1}{A} [Bf_2(A) - Af_2(B)] \quad (11)$$

$$C = t(1 + E_1 - E_2) \left\{ \left(1 + \frac{y^2}{2t} \right) \operatorname{erfc} \left(\frac{y}{2\sqrt{t}} \right) - \frac{ye^{-\frac{y^2}{4t}}}{\sqrt{\pi t}} \right\} + \frac{\xi}{2(A - B)} [f_1(A, -i\omega) + f_1(A, i\omega) - f_1(B, -i\omega) - f_1(B, i\omega)] - \frac{E_1}{A} [Bf_2(A) - Af_2(B)] \quad (12)$$

For the sake of succinctness, our study refers to the situation where pressure work is omitted and the environment is isothermal ($\gamma = 0, \xi = 0$) as the classical scenario. The velocity (u^*), temperature (θ^*) and concentration (C^*) profiles for classical case are obtained as,

$$u^* = \frac{1}{2} [f_1(N, -i\omega) + f_1(N, i\omega)] - D_3 f_2(N) + tD_3 \left[\left(1 + \frac{y^2}{2t} \right) \operatorname{erfc} \left(\frac{y}{2\sqrt{t}} \right) - \frac{ye^{-\frac{y^2}{4t}}}{\sqrt{\pi t}} \right] \quad (13)$$

$$\theta^* = t \left[\left(1 + \frac{y^2}{2t} \right) \operatorname{erfc} \left(\frac{y}{2\sqrt{t}} \right) - \frac{ye^{-\frac{y^2}{4t}}}{\sqrt{\pi t}} \right] \quad (14)$$

$$C^* = t \left[\left(1 + \frac{y^2}{2t} \right) \operatorname{erfc} \left(\frac{y}{2\sqrt{t}} \right) - \frac{ye^{-\frac{y^2}{4t}}}{\sqrt{\pi t}} \right] \quad (15)$$

where

$$N = M + \frac{1}{Da}, \quad A = \frac{N + \sqrt{N^2 - 4\gamma Gr - 4\xi Gc}}{2}, \quad B = \frac{N - \sqrt{N^2 - 4\gamma Gr - 4\xi Gc}}{2}, \quad C_1 = \frac{A}{2(A - B)},$$

$$C_2 = \frac{B}{2(A - B)}, \quad C_3 = \frac{Gr + Gc}{A - B}, \quad D_1 = \frac{\gamma(Gr + Gc)}{A(A - B)}, \quad D_2 = \frac{\gamma(Gr + Gc)}{B(A - B)}, \quad D_3 = \frac{Gr + Gc}{N},$$

$$E_1 = \frac{\xi(Gr + Gc)}{A(A - B)}, \quad E_2 = \frac{\xi(Gr + Gc)}{B(A - B)}, \quad E_3 = \frac{\gamma}{2(A - B)}, \quad E_4 = \frac{\xi}{2(A - B)}.$$

And f_i 's are inverse Laplace transforms and are given by

$$f_1(A, i\omega) = L^{-1} \left\{ \frac{e^{-y\sqrt{s+A}}}{s + i\omega} \right\} \text{ and } f_2(A) = L^{-1} \left\{ \frac{e^{-y\sqrt{s+A}}}{s^2} \right\}$$

Using the formulas given by [19], we separate the complex arguments of the error function that were present in the preceding expressions into real and imaginary components.

2.2. Skin-Friction

The following provides non-dimensional computation of skin-friction of the plate:

$$\tau = - \frac{du}{dy} \Big|_{y=0} \quad (16)$$

Now from equation (10) we get the expression for skin-friction as,

$$\tau = C_1 \left[e^{i\omega t} \left(\sqrt{A + i\omega} \right) \operatorname{erf} \left(\sqrt{(A + i\omega)t} \right) + e^{-i\omega t} \left(\sqrt{A - i\omega} \right) \operatorname{erf} \left(\sqrt{(A - i\omega)t} \right) + \frac{2e^{-At}}{\sqrt{\pi t}} \right] -$$

$$C_2 \left[e^{i\omega t} (\sqrt{B+i\omega}) \operatorname{erf}(\sqrt{(B+i\omega)t}) + e^{-i\omega t} (\sqrt{B-i\omega}) \operatorname{erf}(\sqrt{(B-i\omega)t}) + \frac{2e^{-Bt}}{\sqrt{\pi t}} \right] -$$

$$C_3 \left[t\sqrt{A} \operatorname{erf}(\sqrt{At}) - t\sqrt{B} \operatorname{erf}(\sqrt{Bt}) + \sqrt{\frac{t}{\pi}} (e^{-At} - e^{-Bt}) + \frac{\operatorname{erf}(\sqrt{At})}{2\sqrt{A}} - \frac{\operatorname{erf}(\sqrt{Bt})}{2\sqrt{B}} \right] \quad (17)$$

Skin-friction in classical scenario is obtained as,

$$\tau^* = \frac{1}{2} \left[e^{i\omega t} (\sqrt{N+i\omega}) \operatorname{erf}(\sqrt{(N+i\omega)t}) + e^{-i\omega t} (\sqrt{N-i\omega}) \operatorname{erf}(\sqrt{(N-i\omega)t}) + \frac{2e^{-Nt}}{\sqrt{\pi t}} \right] -$$

$$D_3 \left[t\sqrt{N} \operatorname{erf}(\sqrt{Nt}) - \sqrt{\frac{t}{\pi}} e^{-Nt} - \frac{\operatorname{erf}(\sqrt{Nt})}{\sqrt{N}} \right] \quad (18)$$

2.3. Plate Heat Flux (Nusselt Number)

The non-dimensional form of rate of heat transfer (Nusselt Number) is given by,

$$Nu = - \left. \frac{d\theta}{dy} \right|_{y=0} \quad (19)$$

Now from equation (11) we get the expression for Nusselt number as,

$$Nu = 2\sqrt{\frac{t}{\pi}} (1 + D_1 - D_2) + E_3 \left[e^{i\omega t} (\sqrt{A+i\omega}) \operatorname{erf}(\sqrt{(A+i\omega)t}) + e^{-i\omega t} (\sqrt{A-i\omega}) \operatorname{erf}(\sqrt{(A-i\omega)t}) \right.$$

$$\left. + \frac{2e^{-At}}{\sqrt{\pi t}} - e^{i\omega t} (\sqrt{B+i\omega}) \operatorname{erf}(\sqrt{(B+i\omega)t}) - e^{-i\omega t} (\sqrt{B-i\omega}) \operatorname{erf}(\sqrt{(B-i\omega)t}) - \frac{2e^{-Bt}}{\sqrt{\pi t}} \right] -$$

$$D_1 \left[t\sqrt{A} \operatorname{erf}(\sqrt{At}) + \sqrt{\frac{t}{\pi}} e^{-At} + \frac{\operatorname{erf}(\sqrt{At})}{2\sqrt{A}} \right] + D_2 \left[t\sqrt{B} \operatorname{erf}(\sqrt{Bt}) + \sqrt{\frac{t}{\pi}} e^{-Bt} + \frac{\operatorname{erf}(\sqrt{Bt})}{2\sqrt{B}} \right] \quad (20)$$

For classical case, Nusselt number is derived as,

$$Nu^* = 2\sqrt{\frac{t}{\pi}} \quad (21)$$

2.4. Sherwood Number

The non-dimensional form of rate of mass transfer (Sherwood Number) is given by,

$$Sh = - \left. \frac{dC}{dy} \right|_{y=0} \quad (22)$$

Now from equation (12) we get the expression for Sherwood number as,

$$Sh = 2\sqrt{\frac{t}{\pi}} (1 + E_1 - E_2) + E_4 \left[e^{i\omega t} (\sqrt{A+i\omega}) \operatorname{erf}(\sqrt{(A+i\omega)t}) + e^{-i\omega t} (\sqrt{A-i\omega}) \operatorname{erf}(\sqrt{(A-i\omega)t}) \right.$$

$$\left. + \frac{2e^{-At}}{\sqrt{\pi t}} - e^{i\omega t} (\sqrt{B+i\omega}) \operatorname{erf}(\sqrt{(B+i\omega)t}) - e^{-i\omega t} (\sqrt{B-i\omega}) \operatorname{erf}(\sqrt{(B-i\omega)t}) - \frac{2e^{-Bt}}{\sqrt{\pi t}} \right] -$$

$$E_1 \left[t\sqrt{A} \operatorname{erf}(\sqrt{At}) + \sqrt{\frac{t}{\pi}} e^{-At} + \frac{\operatorname{erf}(\sqrt{At})}{2\sqrt{A}} \right] + E_2 \left[t\sqrt{B} \operatorname{erf}(\sqrt{Bt}) + \sqrt{\frac{t}{\pi}} e^{-Bt} + \frac{\operatorname{erf}(\sqrt{Bt})}{2\sqrt{B}} \right] \quad (23)$$

For classical case, Sherwood number is derived as,

$$Sh^* = 2\sqrt{\frac{t}{\pi}} \tag{24}$$

3. RESULTS AND DISCUSSIONS

The solutions from the preceding section are shown in Figures from 2 to 18 after being numerically computed to talk about how the temperature, velocity, concentration fields, skin-friction, Nusselt number and Sherwood number are influenced by different physical parameters. This provides us with better understanding of the problem in case of physical significance. It has been found that a stratified fluid moves more slowly than an equivalent volume of an unstratified fluid. For various values of magnetic parameter M , Darcy number Da , thermal Grashof number Gr , mass Grashof number Gc , Figures 2 to 9 represent the velocity profiles. It has been observed that while increasing the magnetic parameter M , velocity profile decreases due to a resistive type of force (Lorentz force) occurs which lowers the flow velocity. While velocity increases as Darcy number Da , thermal Grashof number Gr and mass Grashof number Gc are increased in both the cases ($\gamma = 0, \xi = 0$) and ($\gamma \neq 0, \xi \neq 0$). The classical velocity increases over time (t), but it stabilizes when stratification is present.

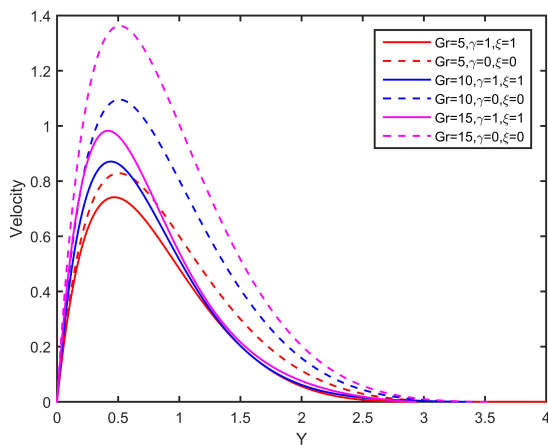


Figure 2. Effects of Gr on Velocity Profile for $t = 1, M = 1, Gc = 10, Da = 0.5, \omega = \frac{\pi}{4}$.

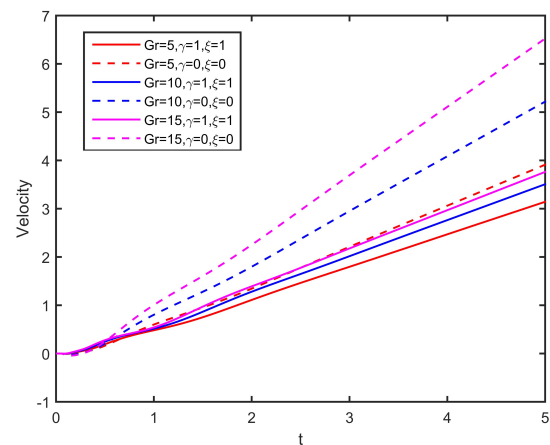


Figure 3. Effects of Gr on Velocity Profile for $y = 1, M = 1, Gc = 10, Da = 0.5, \omega = \frac{\pi}{4}$.

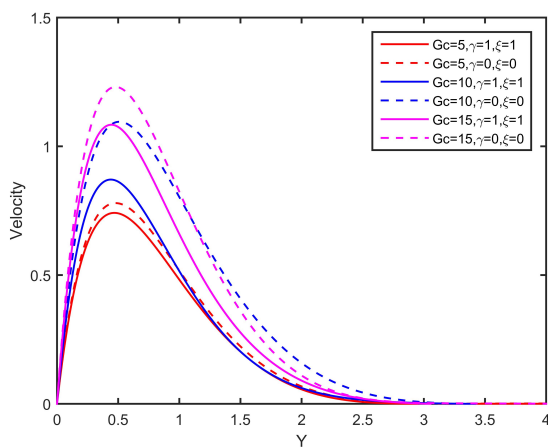


Figure 4. Effects of Gc on Velocity Profile for $t = 1, M = 1, Gr = 10, Da = 0.5, \omega = \frac{\pi}{4}$.

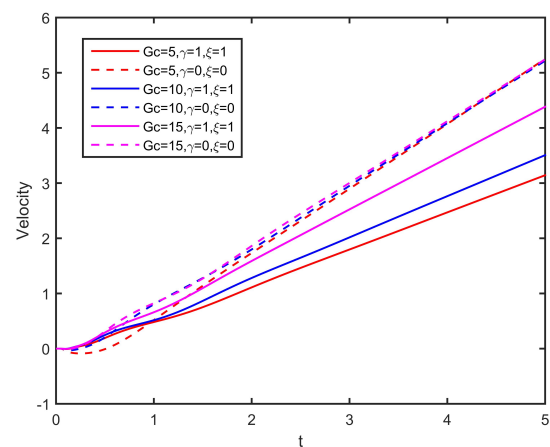


Figure 5. Effects of Gc on Velocity Profile for $y = 1, M = 1, Gr = 10, Da = 0.5, \omega = \frac{\pi}{4}$.

The effects of Gr and Gc on temperature profile are seen in Figures (10) and (11). Temperature increases as Gr and Gc increase and decreases as Gr and Gc decrease simultaneously. The effects of magnetic parameter M on temperature profile are depicted in the Figures 12 and 13. Temperature increases as M increases and decreases with decreasing the

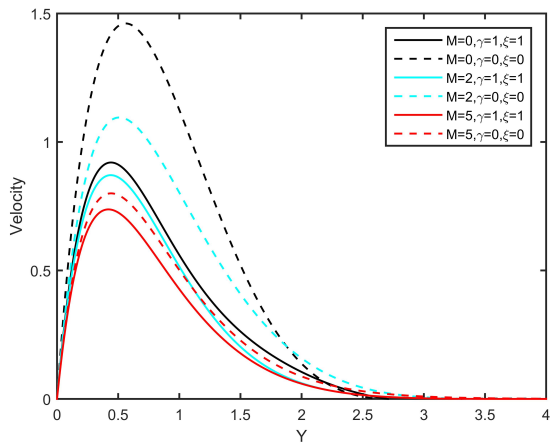


Figure 6. Effects of M on Velocity Profile for $t = 1$, $Gr = 10$, $Gc = 10$, $Da = 0.5$, $\omega = \frac{\pi}{4}$.

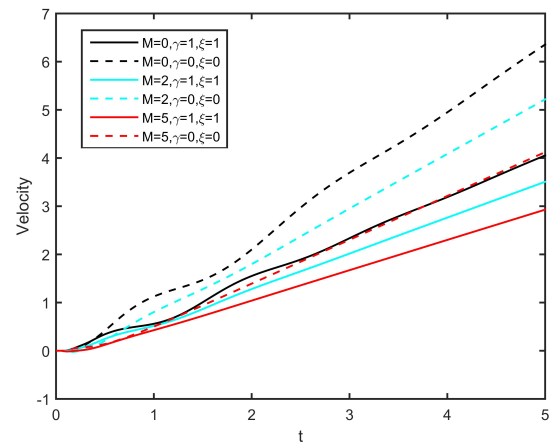


Figure 7. Effects of M on Velocity Profile for $y = 1$, $Gr = 10$, $Gc = 10$, $Da = 0.5$, $\omega = \frac{\pi}{4}$.

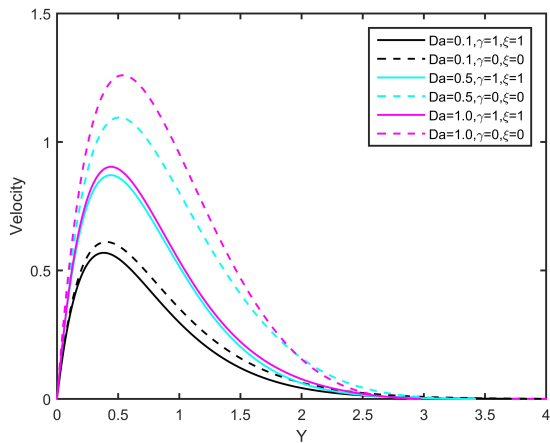


Figure 8. Effects of Da on Velocity Profile for $t = 1$, $Gr = 10$, $Gc = 10$, $M = 1$, $\omega = \frac{\pi}{4}$.

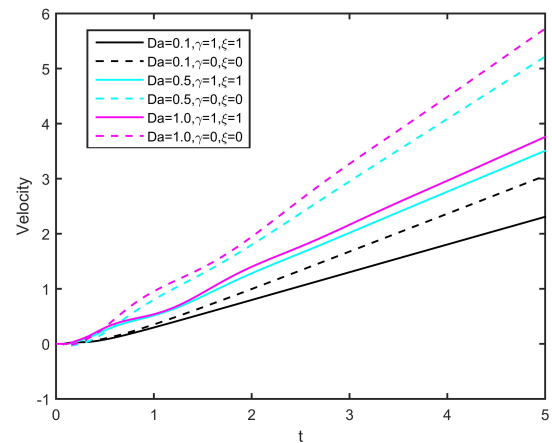


Figure 9. Effects of Da on Velocity Profile for $y = 1$, $Gr = 10$, $Gc = 10$, $M = 1$, $\omega = \frac{\pi}{4}$.

magnetic parameter M . In our study it has been found that temperature is more in classical case as compared to the case

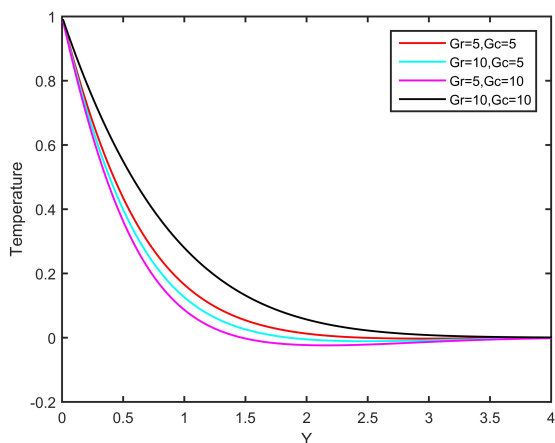


Figure 10. Effects of Gr and Gc on Temperature Profile for $t = 1$, $\gamma = 1$, $\xi = 1$, $M = 1$, $Da = 0.5$, $\omega = \frac{\pi}{4}$.

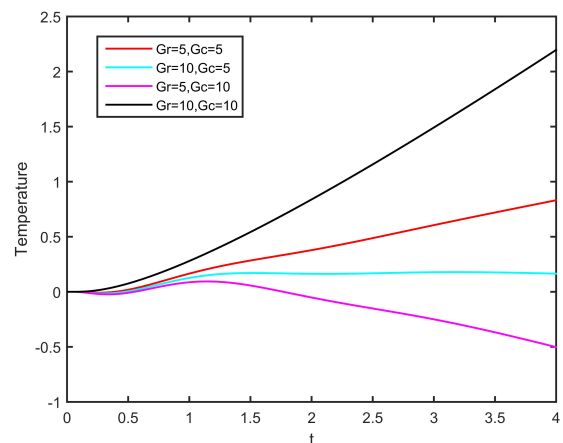


Figure 11. Effects of Gr and Gc on Temperature Profile for $y = 1$, $\gamma = 1$, $\xi = 1$, $M = 1$, $Da = 0.5$, $\omega = \frac{\pi}{4}$.

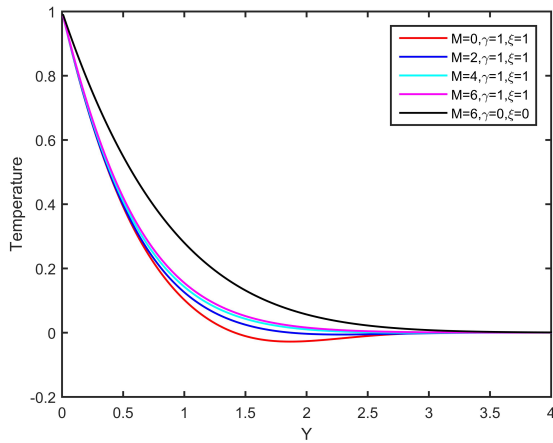


Figure 12. Effects of M on Temperature Profile for $t = 1$, $Gr = 10$, $Gc = 10$, $M = 1$, $Da = 0.5$, $\omega = \frac{\pi}{4}$.

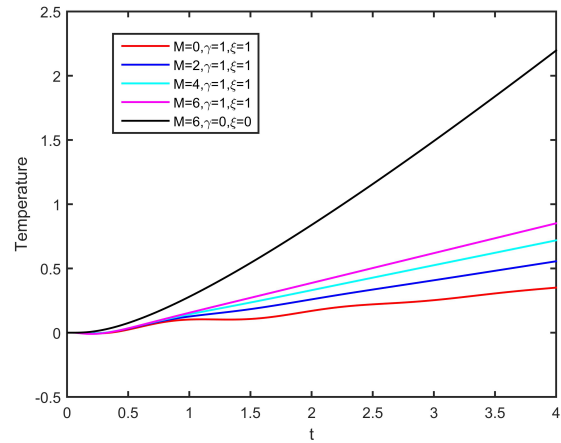


Figure 13. Effects of M on Temperature Profile for $y = 1$, $Gr = 10$, $Gc = 10$, $M = 1$, $Da = 0.5$, $\omega = \frac{\pi}{4}$.

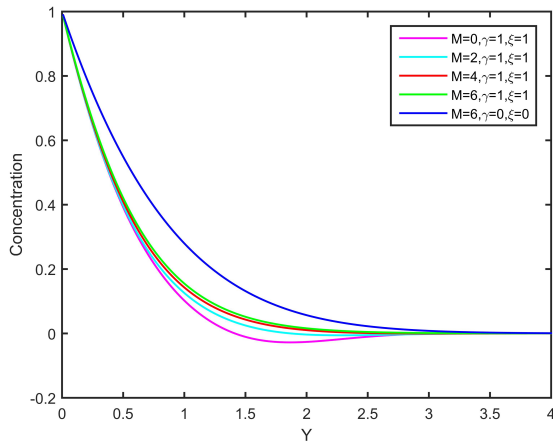


Figure 14. Effects of M on Concentration Profile for $t = 1$, $Gr = 10$, $Gc = 10$, $Da = 0.5$, $\omega = \frac{\pi}{4}$.

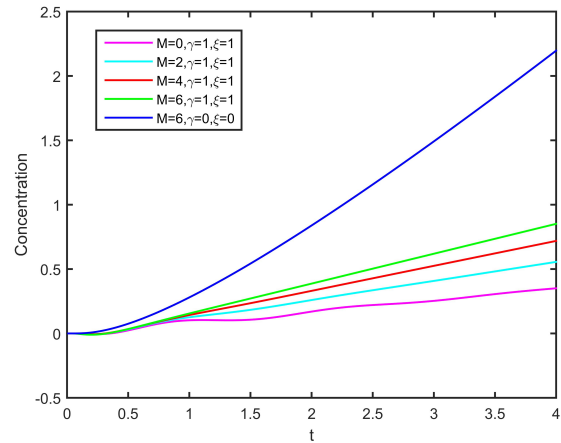


Figure 15. Effects of M on Concentration Profile for $y = 1$, $Gr = 10$, $Gc = 10$, $Da = 0.5$, $\omega = \frac{\pi}{4}$.

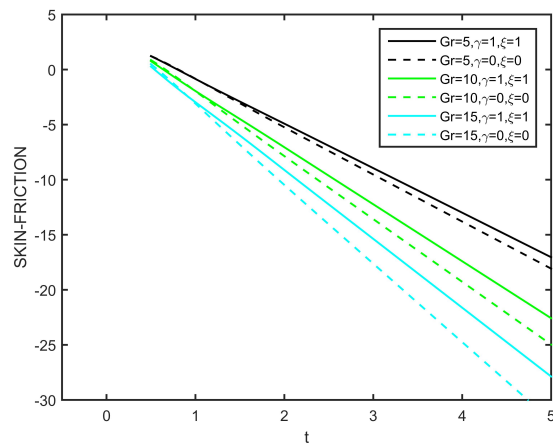


Figure 16. Effects of Gr on Skin-Friction Profile for $y = 1$, $Gc = 10$, $Da = 0.5$, $\omega = \frac{\pi}{4}$.

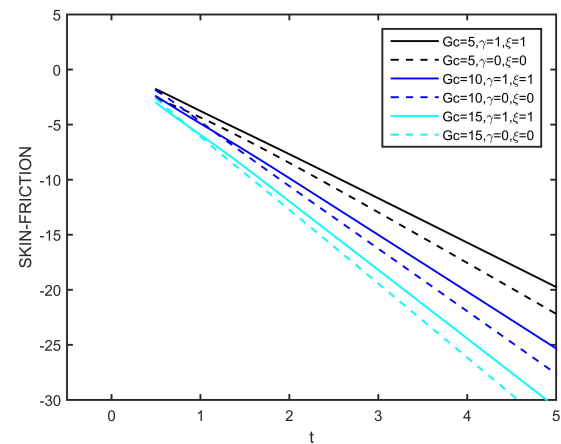


Figure 17. Effects of Gc on Skin-Friction Profile for $y = 1$, $Gr = 10$, $Da = 0.5$, $\omega = \frac{\pi}{4}$.

of stratification. This happens due to the fluid velocity decreases with increase in magnetic parameter M , therefore heat will not easily be convected, as a result this in turn increases the temperature of the fluid. Figure (14) and 15 depicted the

effects of magnetic parameter M on concentration profile. Concentration increases as M increases but in classical case M has no influence on concentration profile.

In contrast to the stratified scenario, our study indicates that the classical instance exhibits more concentration. Figures (16) to (18) illustrated the effects of Gr , Gc and M on skin-friction profile. It has been observed that skin-friction increases with increase in magnetic parameter M while decreases as Gr and Gc are increased in both the cases ($\gamma \neq 0, \xi \neq 0$) and ($\gamma = 0, \xi = 0$). From 2 we can conclude that Nusselt number rise in proportion to increase in Gr and Gc but as M rises, Nusselt number decreases. While increasing the Darcy number, Nusselt number also increases. Sherwood number increases in direct proportion to Gr and Gc declines. In proportion to increase in M and Da , Sherwood number grows.

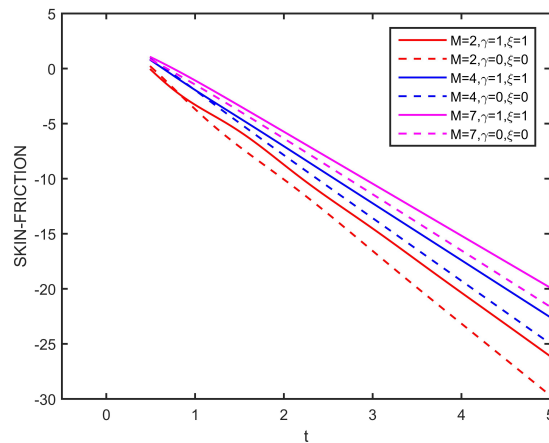


Figure 18. Effects of M on Skin-Friction Profile for $\gamma = 1$, $Gr = 10$, $Gc = 10$, $Da = 0.5$, $\omega = \frac{\pi}{4}$.

Table 1. The impact of different parameters on Sherwood number with $t = 1$, $\omega = \frac{\pi}{4}$.

γ	ξ	Gr	Gc	M	Da	Sh
1	1	10	10	1	0.5	1.4732
0	0	10	10	1	0.5	1.1227
1	1	5	5	1	0.5	1.5896
1	1	10	10	2	0.5	1.6458
1	1	10	10	1	1	1.6593

Table 2. The impact of different parameters on Nusselt number with $t = 1$, $\omega = \frac{\pi}{4}$.

γ	ξ	Gr	Gc	M	Da	Nu
1	1	10	10	1	0.5	1.6544
0	0	10	10	1	0.5	1.1227
1	1	5	5	1	0.5	1.6011
1	1	10	10	2	0.5	1.6466
1	1	10	10	1	1	1.6597

4. CONCLUSION

We have studied the impact of thermal and mass stratification on MHD flow past an oscillating vertical plate embedded in a porous medium with variable surface conditions. The results of our investigation are contrasted with the scenario in which stratification does not exist. The following are the findings of our investigation:

- For both ($\gamma = 0, \xi = 0$) and ($\gamma \neq 0, \xi \neq 0$), velocity falls as magnetic parameter M increases. In contrast to the stratified scenario, velocity is higher in the classical instance.
- For both the situation of ($\gamma = 0, \xi = 0$) and ($\gamma \neq 0, \xi \neq 0$), velocity grows with increasing Darcy number Da . Nonetheless, in contrast to the stratified situation, velocity is higher in the classical case.

- In the cases of ($\gamma = 0, \xi = 0$) and ($\gamma \neq 0, \xi \neq 0$), velocity increases with increase in the thermal (Gr) and mass Grashof (Gc) numbers. But in the classical scenario, velocity is higher than in the stratified case.
- Temperature grows as the magnetic parameter (M) increases and while increasing Gr and Gc , temperature rises. Temperature is higher in classical situation than in the combined stratified environment.
- Concentration rises with rising in the magnetic parameter M . In contrast to the stratified instance, the classical situation ($\gamma = 0, \xi = 0$) involves more concentration.
- Skin-friction decreases as Gr and Gc increases, but increases as M increases, while skin-friction is more in case of stratification.
- In the presence of stratification, the plate heat flux falls with increasing the magnetic parameter M but it grows while increasing the values of Gr, Gc and Da . In contrast to the stratified situation, heat flux is reduced in the classical case.
- The mass flux increases as M, Da, Gr and Gc increase in presence of stratification. However, in classical case, mass flux decreases as compared to the case of stratification.

ORCID

 Pappu Das, <https://orcid.org/0009-0007-8006-3659>;  Rudra Kanta Deka, <https://orcid.org/0009-0007-1573-4890>

REFERENCES

- [1] V.M. Soundalgekar, U.N. Das, and R.K. Deka, "Free convection effects on MHD flow past an infinite vertical oscillating plate with constant heat flux," *Indian J. Math.* **39**, 195-202 (1997).
- [2] J.S Park, and J.M. Hyun, "Transient behavior of vertical buoyancy layer in a stratified fluid," *Intl. J. Heat Mass Transfer*, **41**, 4393-4397 (1998). [https://doi.org/10.1016/S0017-9310\(98\)00175-6](https://doi.org/10.1016/S0017-9310(98)00175-6)
- [3] U.N. Das, R.K. Deka, and V.M. Soundalgekar, "Transient free convection flow past an infinite vertical plate with periodic temperature variation," *J. Heat Transfer*, **121**, 1091-1094 (1999). <https://doi.org/10.1115/1.2826063>
- [4] J.S. Park, "Transient buoyant flows of a stratified fluid in a vertical channel," *KSME. Intl. J.* **15**, 656-664 (2001). <https://doi.org/10.1007/BF03184382>
- [5] A. Shapiro, and E. Fedorovich, "Unsteady convectively driven flow along a vertical plate immersed in a stably stratified fluid," *J. Fluid Mech.* **498**, 333-352 (2004). <https://doi.org/10.1017/S0022112003006803>
- [6] E. Magyari, I. Pop, and B. Keller, "Unsteady free convection along an infinite vertical flat plate embedded in a stably stratified fluid- saturated porous medium," *Transport in Porous Media*, **62**, 233-249 (2006). <https://doi.org/10.1007/s11242-005-1292-6>
- [7] C.Y. Cheng, "Double-diffusive natural convection along a vertical wavy truncated cone in non-newtonian fluid saturated porous media with thermal and mass stratification," *Int. Commun. Heat Mass Transf.* **35**(8), 985-990 (2008). <https://doi.org/10.1016/j.icheatmasstransfer.2008.04.007>
- [8] R.C. Chaudhary, and A. Jain, "MHD heat and mass diffusion flow by natural convection past a surface embedded in a porous medium," *Theoret. Appl. Mech.* **36**(1), 1-27 (2009). <http://dx.doi.org/10.2298/TAM0901001C>
- [9] C.Y. Cheng, "Combined heat and mass transfer in natural convection flow from a vertical wavy surface in a power-law fluid saturated porous medium with thermal and mass stratification," *Int. Commun. Heat Mass Transf.* **36**(4), 351-356 (2009). <http://dx.doi.org/10.1016/j.icheatmasstransfer.2009.01.003>
- [10] B.C. Neog, and R.K. Deka, "Unsteady natural convection flow past an accelerated vertical plate in a thermally stratified fluid," *Theoret. Appl. Mech.* **6**(4), 261-274 (2009). <https://doi.org/10.2298/TAM0904261D>
- [11] S. Gurminder, P.R. Sharma, and A.J. Chamkha, "Effect of thermally stratified ambient fluid on MHD convective flow along a moving nonisothermal vertical plate, *Intl. J. Phy. Sci.* **5**(3), 208-215 (2010). <https://doi.org/10.5897/IJPS.9000199>
- [12] R.K. Deka, and A. Bhattacharya, "Magneto-Hydrodynamic (MHD) flow past an infinite vertical plate immersed in a stably stratified fluid," *International Journal of the Physical Sciences*, **6**(24), 5831-5836 (2011). <https://doi.org/10.5897/IJPS11.011>
- [13] R. Muthucumaraswamy, and V. Visalakshi, "Radiative flow past an exponentially accelerated vertical plate with variable temperature and mass diffusion," *Int. J. of Enng. Annals. of Faculty Engineering Hunedoara*, **9**, 137-140 (2011). <https://annals.fih.upt.ro/pdf-full/2011/ANNALS-2011-2-26.pdf>
- [14] A.G.V. Kumar, S.V.K. Varma, and R. Mohan, "Chemical reaction and radiation effects on MHD free convective flow past an exponentially accelerated vertical plate with variable temperature and variable mass diffusion," *Annals of the Faculty of Engineering Hunedoara*, **10**(2), 195 (2012). <https://annals.fih.upt.ro/pdf-full/2012/ANNALS-2012-2-32.pdf>
- [15] R.K. Deka, and A. Paul, "Convectively driven flow past an infinite moving vertical cylinder with thermal and mass stratification," *Pramana*, **81**, 641-665 (2013). <http://dx.doi.org/10.1007/s12043-013-0604-6>

- [16] H. Kumar, and R.K. Deka, "Thermal and mass stratification effects on unsteady flow past an accelerated infinite vertical plate with variable temperature and exponential mass diffusion in porous medium," East European Journal of Physics, (4), 87-97 (2023). <https://doi.org/10.26565/2312-4334-2023-4-09>
- [17] R.S. Nath, and R.K. Deka, "Thermal and mass stratification effects on unsteady parabolic flow past an infinite vertical plate with exponential decaying temperature and variable mass diffusion in porous medium," ZAMM-Journal of Applied Mathematics and Mechanics/Zeitschrift für Angewandte Mathematik und Mechanik, **104**(6), e202300475 (2024). <http://dx.doi.org/10.1002/zamm.202300475>
- [18] R.S. Nath, R.K. Deka, "Thermal and mass stratification effects on MHD nanofluid past an exponentially accelerated vertical plate through a porous medium with thermal radiation and heat source," Int J Mod Phys B, 2550045. In press (2024). <https://doi.org/10.1142/S0217979225500456>
- [19] R.S. Nath, R.K. Deka, "Theoretical study of thermal and mass stratification effects on MHD nanofluid past an exponentially accelerated vertical plate in a porous medium in presence of heat source, thermal radiation and chemical reaction," Int J Appl Comput Math, **10**(2): 92 (2024). <https://doi.org/10.1007/s40819-024-01721-9>
- [20] P. Das, R.K. Deka, "Thermal and mass stratification effects on unsteady MHD parabolic flow past an infinite vertical plate with variable temperature and mass diffusion through porous medium," East European Journal of Physics, 2: 181-191 (2024). <https://doi.org/10.26565/2312-4334-2024-2-17>
- [21] D. Sahu, R.K. Deka, "Thermal and mass stratification effects on MHD flow past an accelerated vertical plate with variable temperature and exponential mass diffusion embedded in a porous medium," East European Journal of Physics, 2: 161-171 (2024). <https://doi.org/10.26565/2312-4334-2024-2-15>
- [22] D. Sahu, R.K. Deka, "Influences of thermal stratification and chemical reaction on MHD free convective flow along an accelerated vertical plate with variable temperature and exponential mass diffusion in a porous medium," Heat Transfer, 2024; 1-24 (2024). <https://doi.org/10.1002/hjt.23106>
- [23] R.B. Hetnarski, "An algorithm for generating some inverse Laplace transforms of exponential form," ZAMP, **26**, 249-253 (1975). <https://doi.org/10.1007/BF01591514>
- [24] M. Abramowitz, I.A. Stegun, and R.H. Romer, "Handbook of mathematical functions with formulas, graphs, and mathematical tables," American Journal of Physics, **56**(10), 958 (1988). <https://doi.org/10.1119/1.15378>

**ВПЛИВ ТЕРМІЧНОЇ ТА МАСОВОЇ СТРАТИФІКАЦІЇ НА НЕСТАЦІОНАРНИЙ МГД-ПОТІК ПОВЗ
ОСЦИЛЮЮЧУ ВЕРТИКАЛЬНУ ПЛАСТИНУ, ВМОНТОВАНУ В ПОРИСТЕ СЕРЕДОВИЩЕ
ЗІ ЗМІННИМИ УМОВАМИ ПОВЕРХНІ**

Паппу Дас, Рудра Канта Дека

Факультет математики, Університет Гаухаті, Гувахаті-781014, Ассам, Індія

Було проведено дослідження того, як теплова та масова стратифікація впливає на магнітогідродинамічний потік повз пластину, яка коливається вертикально навколо своєї власної осі, в яку вона занурена в пористе середовище зі змінною дифузійною теплою та масою. Для полів концентрації, температури та швидкості безрозмірні керівні рівняння розв'язуються за допомогою методу перетворення Лапласа для унітарних чисел Прандтля та Шмідта, коли пластина гармонійно коливається у власній площині. Числові обчислення проводяться та представлені у вигляді графіків для різних фізичних параметрів, таких як теплове число Грасгофа, фазовий кут, масове число Грасгофа, параметр стратифікації та час на концентрацію, швидкість, температуру, тепловий потік пластини, потік маси та тертя шкіри. Результати цього дослідження можуть бути використані для покращення розуміння потоку МГД на вертикальній коливальній пластині в комбінованих стратифікованих середовищах. Значні висновки, що впливають із масової та термічної стратифікації, порівнюються зі сценарієм, у якому стратифікація відсутня.

Ключові слова: МГД потік; коливальна пластина; електропровідна рідина; нестабільний потік; термічна стратифікація; масове розширення; пористе середовище